

Flux-Flow Resistance in Type-II Superconductors

Y. B. KIM, C. F. HEMPSTEAD, AND A. R. STRNAD

Bell Telephone Laboratories, Murray Hill, New Jersey

(Received 18 March 1965)

Electrical resistance of type-II superconductors measured by a dc method is related to the motion of Abrikosov vortices. Flux lines in the mixed state are driven into a viscous-flow state by increasing the Lorentz force $\mathbf{J} \times \mathbf{H}$ beyond the depinning threshold; the voltage observed under this condition is linear in current and the slope $\Delta V/\Delta I$ is interpreted to represent the flow rate. At low temperatures, the flow resistivity ρ_f so measured follows an empirical relation $\rho_f/\rho_n = H/H_{c2}$, where ρ_n is the normal-state resistivity and H_{c2} the upper critical field predicted by the Ginsburg-Landau-Abrikosov-Gor'kov (GLAG) theory. In high-field superconductors the GLAG upper critical fields are not accessible for conventional measurements since the paramagnetic spin alignment quenches superconductivity at much lower fields, but the above empirical rule still holds and makes it possible to determine the GLAG upper critical fields from the flow-resistivity measurements. The empirical relation also suggests that the frictional drag on a moving flux line arises from normal currents flowing in the core of the vortex line. The observed damping is, however, much larger than can be accounted for by eddy currents induced by the moving magnetic field of the vortex line. Two new mechanisms, one proposed by Tinkham and another by Stephen and Bardeen, appear to correct this difficulty and they are discussed in the text. Also reported is a new type of resistance-minimum phenomenon: if the temperature T is increased from zero at a fixed field H , the resistance $R(T)$ of a type-II specimen decreases initially and goes through a minimum before it reaches the normal resistance at $T_c(H)$. This behavior is qualitatively accounted for by including the dissipation outside of the vortex core.

I. INTRODUCTION

AT present, the microscopic description of hard superconductivity is based primarily on the Ginsburg-Landau-Abrikosov-Gor'kov (GLAG) theory.¹ This theory attained its prominence shortly after the discovery by Kunzler *et al.*² of the technologically important high-field superconductors. Goodman³ was first to point out the relevance of the GLAG theory to high-field superconductivity, and subsequent experimental verifications, particularly by Berlincourt and Hake,⁴ have rendered convincing support to the theory. Superconductors having coherence length ξ smaller than the penetration depth λ follow the GLAG description and they are now categorized as type II, in contrast to the type I that represents ideal soft superconductors. Central to the theory of type-II superconductors is Abrikosov's characterization of the mixed state as a lattice-like structure of quantized flux lines, or vortices of superelectrons. The core of a vortex is essentially in the normal state and is usually approximated by a cylinder of normal metal of radius $\sim \xi$. Outside the core the type-I behavior prevails and the magnetic field is screened by the circulating superelectrons to a distance $\sim \lambda$. Since each flux line contains one flux quantum $\varphi_0 = hc/2e$, the density of flux lines n determines the magnetic induction $B = n\varphi_0$.

Although Abrikosov's description of the mixed state

is concerned strictly with an equilibrium situation, the structure of individual flux lines is fairly rigid and plays an important role in many nonequilibrium phenomena. In fact, such concepts⁵ as flux pinning, flux creep, and flux flow, that have been very useful in the understanding of hard superconductivity, all envisage the motion of Abrikosov flux lines. Here the nonequilibrium situation is created in the specimen by the presence of a transport current \mathbf{J} ; the density of flux lines is no longer uniform and the lines are subject to a driving force exerted by the magnetic pressure gradient, or the Lorentz force.⁶⁻⁸ Thus in an ideal type-II superconductor the flux lines are expected to move in such a direction as to equalize the magnetic pressure. In practice, of course, lattice defects of various kinds present in the material effectively pin down the flux lines and enable the specimen to sustain nonuniform flux-line densities. The "critical state"^{9,10} of hard superconductors specifies the threshold beyond which the pinning force is overcome by the Lorentz force and a static configuration of flux structure no longer exists. According to the flux-creep theory of Anderson,⁸ however, the flux pinning is not absolutely rigid even below this threshold: at a finite temperature, flux lines are slowly moving past the pinning centers because of thermal activation.

The realization that flux lines can only move *dissipatively* marked an important step to the present

¹ V. L. Ginsburg and L. D. Landau, *Zh. Eksperim. i Teor. Fiz.* **20**, 1064 (1950); A. A. Abrikosov, *ibid.* **32**, 1442 (1957) [English transl.: *Soviet Phys.—JETP* **5**, 1174 (1957)]; L. P. Gor'kov, *ibid.* **37**, 1407 (1959) [English transl.: *Soviet Phys.—JETP* **10**, 998 (1960)].

² J. E. Kunzler, E. Buehler, F. S. L. Hsu, and J. H. Wernick, *Phys. Rev. Letters* **6**, 89 (1961).

³ B. B. Goodman, *IBM J. Res. Develop.* **6**, 63 (1962).

⁴ T. G. Berlincourt and R. R. Hake, *Phys. Rev. Letters* **7**, 293 (1962); *Phys. Rev.* **131**, 140 (1963).

⁵ P. W. Anderson and Y. B. Kim, *Rev. Mod. Phys.* **36**, 39 (1964).

⁶ C. J. Gorter, *Phys. Letters* **1**, 69 (1962); **2**, 26 (1962).

⁷ Y. B. Kim, C. F. Hempstead, and A. R. Strnad, *Phys. Rev. Letters* **9**, 306 (1962).

⁸ P. W. Anderson, *Phys. Rev. Letters* **9**, 309 (1962).

⁹ C. P. Bean, *Phys. Rev. Letters* **8**, 250 (1962).

¹⁰ Y. B. Kim, C. F. Hempstead, and A. R. Strnad, *Phys. Rev.* **129**, 528 (1963).

understanding of hard superconductivity. Specifically, it was proposed¹¹ that moving flux lines induce electric fields, presumably by the induction mechanism $\nabla \times \mathbf{E} = -c^{-1} \partial \mathbf{B} / \partial t$. This is a significant departure from the London concept of $\mathbf{E} = 0$ in type-I superconductors. The presence of electric fields clearly implies power dissipation $P = \mathbf{E} \cdot \mathbf{J}$ in hard superconductors and leads to severe thermal instabilities when the flux lines are forced to move against large and irregular pinning forces. Bizarre instability phenomena encountered in superconducting magnets originate from such thermal instabilities, but our understanding in this area remains largely qualitative. The more fundamental aspect of the dissipative processes associated with moving flux lines has been clarified considerably from the study of what is called the "flux-flow" state.¹¹⁻¹³ If the specimen is made thermally stable, it can be driven into a state wherein the Lorentz driving force exceeds the pinning force and the flux lines undergo a viscous flow. The significance of this phenomenon lies in the fact that the flow rate is independent of pinning and is determined by the bulk superconducting properties of the material. From a systematic investigation of low-field type-II superconductors, we have derived remarkably simple empirical relation¹⁴ which suggests that at low temperatures the dissipation is confined to the core region of a moving vortex line, but the electric field is much larger than that implied by the simple induction mechanism.

The motion of flux lines clearly involves a time variation of the order parameter and a complete solution of the problem requires time-dependent generalizations of the GLAG theory. However, since the vortex structure is fairly rigid and the relevant motion is slow enough, some sort of model calculations may be possible in lieu of the general theory. In fact, several such theoretical models¹⁵⁻¹⁷ have recently been proposed to account for the empirical results. In this paper, the experimental data will be presented in comparison with these theoretical models. We also report measurements extended to high-field superconducting alloys for which the observed upper critical fields are limited by Pauli spin paramagnetic susceptibility. In these alloys the flux-flow measurements enable us to determine the hypothetical upper critical fields predicted by the GLAG theory.

¹¹ Y. B. Kim, C. F. Hempstead, and A. R. Strnad, Phys. Rev. **131**, 2486 (1963).

¹² Y. B. Kim, C. F. Hempstead, and A. R. Strnad, Rev. Mod. Phys. **36**, 43 (1964).

¹³ C. F. Hempstead and Y. B. Kim, Phys. Rev. Letters **12**, 145 (1964).

¹⁴ A. R. Strnad, C. F. Hempstead, and Y. B. Kim, Phys. Rev. Letters **13**, 794 (1964).

¹⁵ M. Tinkham, Phys. Rev. Letters **13**, 804 (1964).

¹⁶ M. J. Stephen and J. Bardeen, Phys. Rev. Letters **14**, 112 (1965).

¹⁷ H. Suhl, Phys. Rev. Letters **14**, 226 (1965).

II. FLOW RESISTIVITY

In this section we review the concept of the flux-flow state that has grown out of our experimental investigations. Consider Abrikosov flux lines in the mixed state of a type-II superconductor (see Fig. 1). We choose a frame such that the magnetic field is in the z direction and the array of vortices is in the x - y plane. The specimen geometry (a flat sheet) is such that $B = n\phi_0 \simeq H$. The transport current J in the x direction generates a gradient in the line density n , so that

$$\frac{\partial B}{\partial y} = \phi_0 \frac{\partial n}{\partial y} = \frac{4\pi}{c} J, \quad (1)$$

$$\frac{\partial}{\partial y} \left(\frac{B^2}{8\pi} \right) = \frac{BJ}{c} = n \frac{\phi_0 J}{c}.$$

If we distribute the *macroscopic* magnetic pressure equally to each flux line, the Lorentz force on each flux line per unit length is given by

$$F_L = J\phi_0/c. \quad (2)$$

As the Lorentz force exceeds the pinning force F_P , the creep-like motion of flux lines changes into a viscous flow characterized by the relation

$$\eta v_L = F_L - F_P, \quad (3)$$

where v_L is the line velocity and $\eta(H, T)$ the viscosity coefficient of the medium. Since a power input is required to maintain a steady state (constant J and v_L), the specimen will develop an observable electric field in the direction of J . We consider this electric field as arising from the motion of flux lines, i.e.,

$$E_0 = n(v_L/c)\phi_0 = (v_L/c)B. \quad (4)$$

This expression refers to the *macroscopic* electric field and makes no specific assumption with regard to the damping mechanism since v_L is determined from (3) through η , which is left as a free parameter. E_0 is, however, required to be proportional to v_L . The pinning effect can be eliminated from the problem by taking

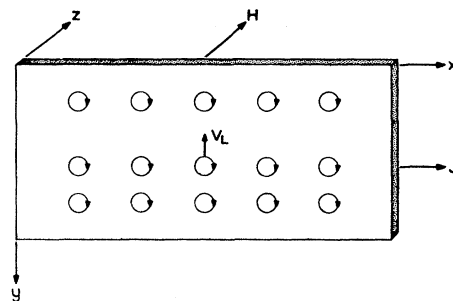


FIG. 1. Schematic representation of a flux-flow state.

derivatives of (3) and (4), i.e.,

$$\frac{dv_L}{dF_L} = \frac{c}{\varphi_0} \frac{dv_L}{dJ} = \frac{1}{\eta}; \quad \frac{dE_0}{dv_L} = \frac{B}{c}.$$

Combining these two expressions, we define the "flow resistivity"

$$\rho_f = \frac{dE_0}{dJ} = \frac{\varphi_0 B}{\eta c^2}. \quad (5)$$

The measurement of ρ_f thus yields the viscosity coefficient η . Note that ρ_f is inversely proportional to η . If the damping of the medium increases, the flux lines move slower and a smaller resistivity results.

A typical example of the experimental determination of flow resistivity is illustrated in Fig. 2. At a fixed external field H , the voltage appearing in the direction of the current is measured as a function of current I . No detectable voltage appears until I exceeds the

critical current. In terms of Eq. (3), the critical current corresponds to the condition where $F_L = F_P$. For $F_L > F_P$, V increases rapidly and becomes linear in I , indicating that $E_0 \propto v_L$ as was assumed in (4). Also note that the slope $\Delta V/\Delta I$ is independent of the critical current of the sample, or the pinning force F_P of (3). In short, the flow resistivity refers to an electrical resistivity that would be observed in the mixed state of a defect-free type-II superconductor. We use the adjective "flow" to emphasize that (a) the resistivity is interpreted as arising from a viscous flow of flux lines, and (b) experimentally a differential resistivity is measured to eliminate the effect of residual defects.

The possible existence of the Magnus force on moving flux lines was first considered by De Gennes and Matricon.¹⁸ The Magnus force is a hydrodynamic lift experienced by a vortex moving in a liquid. By treating the flux line as moving through a medium of free electrons, they derived an expression

$$\mathbf{F}_M = Ne(v_L/c) \times \varphi_0, \quad (6)$$

where N is the electron concentration. Balanced against the line tension, this force could give rise to transverse vibrational modes. No such modes have yet been detected experimentally. Another consequence of the Magnus force was pointed out by Vinen.¹⁹ In the absence of drag the line may move, like a vortex in superfluid helium, not in the direction of the applied force but perpendicular to it. In the flux line configuration of Fig. 1, the lines would move in the x direction with $v_L = J/N|e|$, so that the resulting Magnus force (6) is identical to the Lorentz force (2). In this case, the electric field will appear in the y direction as a Hall voltage. When the medium is dissipative, the flux line will move in such a direction as to give a Hall angle

$$\theta = E_{0y}/E_{0x} = Ne\varphi_0/(\eta c). \quad (7)$$

The presence of a Hall voltage has been checked using the specimen geometry shown in Fig. 2. In many samples we do observe voltages transverse to J , but they are not of the Hall type. A typical example is shown in Fig. 3. If we use the empirical expression (15a) for η , the Hall angle expression (7) reduces to $\theta \simeq E_F/\Delta_{00}$ where E_F is the Fermi energy and Δ_{00} the gap parameter at zero field and zero temperature. The possibility of such a large Hall angle is clearly ruled out in the present samples. The situation could be different in clean samples; but Bardeen²⁰ has pointed out that the theoretical arguments for the Magnus force are in error in that the effect of the positive ion background is not taken into account. (*Note added in proof.* More

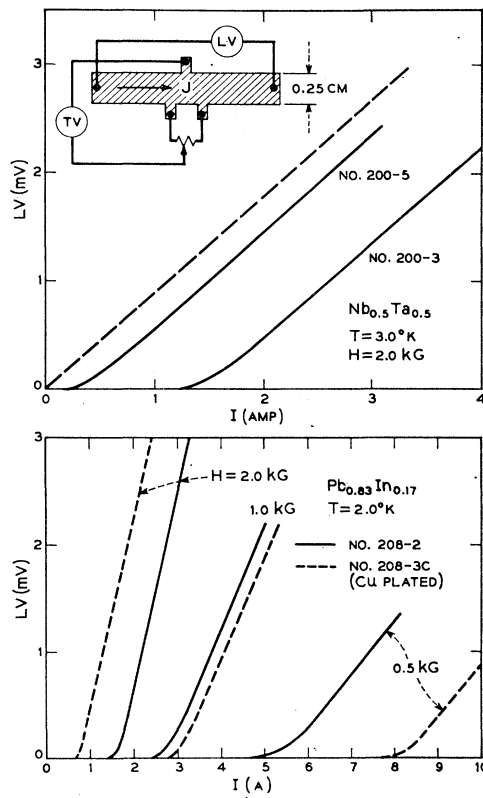


FIG. 2. Voltage-versus-current characteristics. The insert of the upper figure shows the geometry of a sheet sample on which voltages in two directions ($\parallel J$ and $\perp J$) are measured. The solid lines are $V(I)$ characteristics of two Nb-Ta samples containing different amounts of defects. Although the critical currents are different for these two samples, the slopes $\Delta V/\Delta I$ in the linear region are the same. The dashed line is the $V(I)$ expected for a defect-free sample. In the lower figure are shown $V(I)$'s for two Pb-In samples: one with copper plating on the surfaces and the other without. The plating apparently alters the pinning conditions in a complicated way, but leaves the flow resistivity practically unchanged.

¹⁸ P. G. De Gennes and J. Matricon, Rev. Mod. Phys. **36**, 45 (1964).

¹⁹ W. F. Vinen, Rev. Mod. Phys. **36**, 48 (1964); P. H. Borchers, C. E. Gough, W. F. Vinen, and A. C. Warren, Phil. Mag. **10**, 349 (1964).

²⁰ J. Bardeen, Phys. Rev. Letters **13**, 747 (1964).

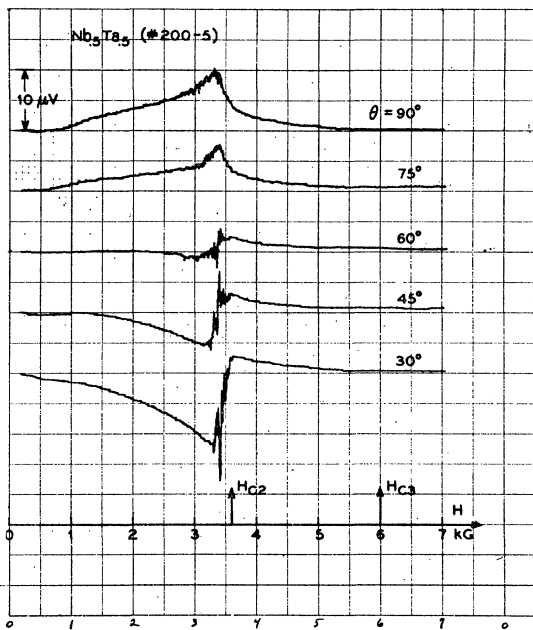


FIG. 3. Transverse voltage characteristics for various orientation of magnetic fields. The transverse voltages observed in the Nb-Ta sample of Fig. 2, with J fixed at 400 A/cm^2 , are shown as a function of H . The magnetic field is rotated around the vertical axis: at $\theta=90^\circ$, $H \perp J$ and $H \perp$ surface; at $\theta=0^\circ$, $H \parallel J$ and $H \parallel$ surface. At $\theta=90^\circ$ the longitudinal voltage increases with H and reaches 2.8 mV at H_{c2} . Note that the transverse voltage reverses at $\theta=30^\circ$, but the phase angle is 60° instead of 180° expected for a Hall-type emf.

recent measurements of the Hall effect in superconductors have been reported by Reed, Fawcett, and Kim, and by Niessen and Staas.^{20a)}

III. DISSIPATIVE MECHANISMS

In an earlier report¹⁴ the flow resistivity of type-II superconducting alloys was shown to follow an approximate law of corresponding states, i.e., ρ_f/ρ_n is independent of alloy composition if expressed as a function of the reduced variables T/T_c and H/H_{c2} . In the limit of $t=T/T_c \rightarrow 0$, the data extrapolate to

$$\rho_f/\rho_n = H/H_{c2}, \tag{8}$$

a result that would follow if the electrical resistance is contributed only by the normal cores and the current does not avoid them.²¹ We made this suggestion by noting that (a) the reduced variable H/H_{c2} represents approximately the fraction of the volume occupied by the vortex cores, and (b) according to Caroli *et al.*²² the

^{20a} W. A. Reed, E. Fawcett, and Y. B. Kim, *Phys. Rev. Letters* **14**, 790 (1965). A. K. Niessen and F. A. Staas, *Phys. Letters* **15**, 26 (1965).

²¹ B. Rosenblum and M. Cardona, *Phys. Rev. Letters* **12**, 657 (1964), have also emphasized this point in their interpretation of the microwave surface resistance of type-II superconductors.

²² C. Caroli, P. G. De Gennes, and J. Martricon, *Phys. Letters* **9**, 307 (1946).

vortex core is practically equivalent to a cylinder of normal metal of radius ξ .

At finite temperatures, the expression (8) is modified to

$$\rho_f/\rho_n = H/[H_{c2}(t)g(t)]. \tag{9}$$

In order to isolate the temperature dependence we write $H_{c2}(t)$ as

$$H_{c2}(t) = H_{c2}(0)h(t). \tag{10}$$

$h(t)$ is available from the calculations by Helfand and Werthamer,²³ and also by Maki.²⁴ We now express (9) in the form:

$$\rho_f/\rho_n = H/[H_{c2}(0)f(t)], \tag{11}$$

where $f(t) = h(t)g(t)$ is unity at $t=0$. At a given H we find ρ_f/ρ_n to be practically independent of t . In other words, empirically $f(t) \approx 1$, or $g(t) \approx 1/h(t)$, so that

$$\rho_f/\rho_n = H/H_{c2}(0). \tag{12}$$

The evidence leading to the empirical relation (12) is illustrated in Fig. 4. Flow-resistivity data on $\text{Nb}_{0.5}\text{Ta}_{0.5}$ are plotted as a function of H at fixed t . In all cases ρ_f/ρ_n starts out linearly in H with a constant slope, i.e., (12) holds for all t 's. Of course, the range of H over which this relation holds decreases rapidly as t increases; at $t=0.33$ (12) holds up to $H/H_{c2} \approx 0.7$. At $t=0$, we may expect this relation to hold all the way up to $H_{c2}(0)$. This extrapolation enables us to obtain $H_{c2}(0) = 8.6 \text{ kG}$ by extending the straight line portion of ρ_f/ρ_n for $t=0.33$. $H_{c2}(0)$ so determined is compared in Fig. 5 with that expected from the measured $H_{c2}(t)$. The solid line is a plot of (10) with $H_{c2}(0) = 8.6 \text{ kG}$ and $h(t)$ given by Helfand and Werthamer.²³ The measured values of $H_{c2}(t)$ indicated by the dots lie practically on

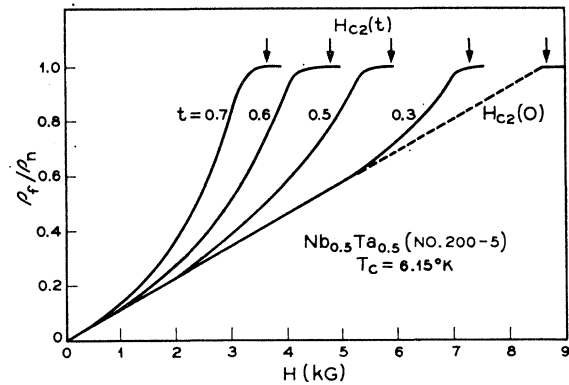


FIG. 4. Flow resistivity versus H and T/T_c . ρ_f/ρ_n of a Nb-Ta specimen is displayed as a function of H at given values of $t=T/T_c$. Vertical arrows indicate the values of $H_{c2}(t)$ measured resistively at $\theta=0^\circ$ orientation. The dashed line indicates the behavior of ρ_f/ρ_n expected at $t=0$. The intersection of this line with $\rho_f/\rho_n = 1$ gives $H_{c2}(0) = 8.6 \text{ kG}$.

²³ E. Helfand and N. R. Werthamer, *Phys. Rev. Letters* **13**, 686 (1964). The $h(t)$ curve shown in Fig. 5 is for $\lambda = 0.882$ $\xi_0/l = 0.5$.

²⁴ K. Maki, *Physics* **1**, 21 (1964); **1**, 127 (1964).

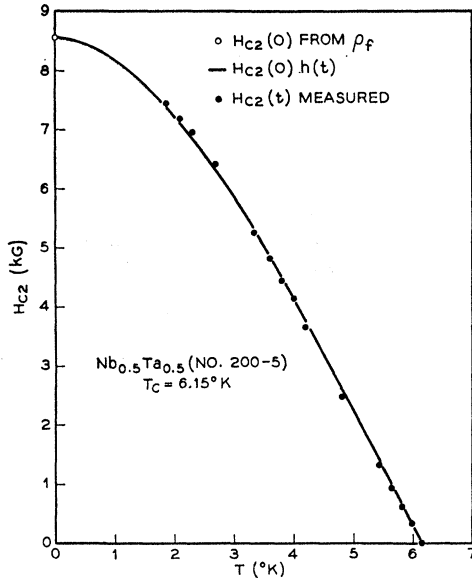


FIG. 5. H_{c2} versus T for a Nb-Ta specimen. The solid curve is derived from the theoretical calculation of Ref. 23 and $H_{c2}(0) = 8.6$ kG determined from the flow resistivity of Fig. 4. $H_{c2}(t)$ measured by the resistive method is shown by the dots.

the calculated curve. This good agreement indicates that the measurement of flow resistivity can effectively be used as a means of determining $H_{c2}(0)$, an application of which will be discussed in Sec. IV.

By combining (5) and (11) with the relation $B \simeq H$, we obtain an empirical expression for the damping coefficient:

$$\eta_{\text{emp}} = (\varphi_0 H_{c2}(0) / \rho_n c^2) f(t); \quad f(t) \simeq 1. \quad (13)$$

In order to relate η_{emp} to other electronic constants of the metal, we take Maki's expression²⁴ for $H_{c2}(0)$ in the dirty limit ($l/\xi_0 \ll 1$) and express it in several alternative ways:

$$H_{c2}(0) = \frac{3}{2} (c \Delta_{00} / e \tau_{\text{col}} v_F) \quad (14)$$

$$= e c \rho_n N(0) \Delta_{00} \quad (14a)$$

$$= 3.1 \times 10^4 \rho_n \gamma T_c; \quad \rho_n \text{ in } \Omega\text{-cm} \quad (14b)$$

$$= 3 \varphi_0 / 2 \pi^2 \xi^2; \quad \xi^2 = \xi_0 l, \quad (14c)$$

where τ_{col} is the collision relaxation time, v_F the Fermi velocity, l the mean free path, $\xi_0 = \hbar v_F / \pi \Delta_{00}$ the BCS coherence length, $N(0)$ the density of states for one spin, γ the electronic specific-heat constant in erg/cm³. By substituting these expressions into (13), we obtain

$$\eta_{\text{emp}} = \varphi_0 H_{c2}(0) / \rho_n c^2 \quad (15)$$

$$= \pi \hbar N(0) \Delta_{00} \quad (15a)$$

$$= 6.4 \times 10^{-12} \gamma T_c \quad (15b)$$

$$= 3 \sigma_n \varphi_0^2 / 2 \pi^2 c^2 \xi^2. \quad (15c)$$

According to (15a) η_{emp} depends on only one basic

normal-state constant $N(0)$ and on the superconducting gap Δ_{00} ; it is manifestly independent of the electronic mean free path l .

We now discuss various dissipative mechanisms that have been proposed to account for the observed damping.

A. Normal Eddy-Current Damping

A moving flux line induces *locally* an electric field

$$\mathbf{E}_i = - (v_L / c) \times \mathbf{H}_i, \quad (16)$$

where \mathbf{H}_i is the magnetic field in the sample. This field may generate normal eddy currents²⁵ and give rise to a dissipation

$$P \equiv n \eta v_L^2 = n \int \int \sigma E^2 dx dy = \frac{n v_L^2}{c^2} \int \int \sigma H_i^2 dx dy,$$

where the integration covers the extension of one flux line. At low temperatures, the dissipation is confined to the vortex core and we obtain

$$\eta = \frac{1}{\rho_n c^2} \int \int_{\text{core}} H_i^2 dx dy \simeq \frac{\xi^2 H_{\text{core}}^2}{\rho_n c^2} = \frac{\varphi_0 H_{c2}(0)}{\rho_n c^2} \left[\frac{H_{\text{core}}}{H_{c2}(0)} \right]^2. \quad (17)$$

This agrees with η_{emp} given by (15) only near H_{c2} ; at low fields the damping given by (17) is far too small to account for the observation. A generalized treatment of the normal eddy-current damping, including the contribution of the noncore region, has been given by Tinkham.¹⁵

B. Relaxation Damping

As an additional source of damping, Tinkham¹⁵ has suggested a relaxation mechanism associated with moving flux lines. As flux lines pass by, the order parameter $\psi(H, T)$ at a given location is forced to oscillate in time between 0 (normal state) and ψ_0 (superconducting) with a frequency $\omega \simeq v_L / \xi$. If it takes a time τ for ψ to approach the instantaneous equilibrium value—that is to say, ψ at a time t is $\psi[H(t - \tau), T]$ instead of the equilibrium value $\psi[H(t), T]$ —the power dissipated in the system will be of order $\langle F \rangle \omega^2 \tau$, where $\langle F \rangle$ is the average energy density. Since the variation in ψ is largely confined to the core region, the appropriate power density is

$$P_\tau = n \pi \xi^2 \langle F \rangle \omega^2 \tau = n \pi \langle F \rangle v_L^2 \tau. \quad (18)$$

For a dirty superconductor, Tinkham proposed to use

$$\tau = (\hbar / \Delta_{00}) [(1 + l^2) / (1 - l^2)]. \quad (19)$$

²⁵ J. Volger, F. A. Staas, and A. G. Van Vijfeijken, Phys. Letters **9**, 303 (1964).

Using the Ginzburg-Landau energy expression for $\langle F \rangle$, and associating Δ_{00} with v_F appearing in the expression of σ_n , he obtained

$$(\rho_f/\rho_n)\tau \simeq (H/H_{c2})[(1-b^2)(1+t^2)]^{-1}, \quad (20)$$

where $b (=B/H_{c2})$ is the fractional volume occupied by the vortex cores. For $b^2 \ll 1$, (20) reduces to (9) with $g(t) = (1+t^2)^2$. Since Tinkham has effectively used $H_{c2}(t) = H_{c2}(0)(1-t^2)(1+t^2)^{-1}$, (20) reduces to (11) with $f(t) = 1-t^4$.

C. Cycloid Damping

If the line velocity is not too large, the structure of a moving vortex is practically undistorted and the vortex electrons execute a cycloidal motion. Stephen and Bardeen¹⁶ pointed out that an electric field, additional to that given by (16), is required to maintain such a motion. If $\mathbf{v}_s(\mathbf{r})$ is the velocity field of a stationary vortex, the electrons in a moving vortex are described by $\mathbf{v}_s(\mathbf{r}-\mathbf{v}_L t)$ and must experience an additional acceleration $\partial \mathbf{v}_s/\partial t = -(\mathbf{v}_L \cdot \nabla)\mathbf{v}_s$. The required electric field is then

$$\mathbf{E}_c = (m/e)(\mathbf{v}_L \cdot \nabla)\mathbf{v}_s. \quad (21)$$

Although $\mathbf{v}_s = 0$ in the vortex core, from the continuity of the potential associated with (21) one obtains an electric field

$$E_c = (v_L/c)(\varphi_0/2\pi\xi^2), \quad (22)$$

which is uniform throughout the core and perpendicular to \mathbf{v}_L . In the flux-line geometry of Fig. 1, this electric field is in the x direction. Since E_c is linear in v_L , the power dissipation in the core $\sigma_n E_c^2 \pi \xi^2$ leads to

$$\eta = \sigma_n \varphi_0^2 / 4\pi c^2 \xi^2. \quad (23)$$

This is approximately one-half of η_{emp} given by (15c), but Stephen and Bardeen point out that dissipation outside of the core may contribute a comparable amount.

Both the relaxation damping and the cycloid damping predict a viscosity coefficient independent of the electronic mean free path and close to η_{emp} . While Tinkham's mechanism depends on relaxation due to the amplitude of the order parameter ψ (proportional to the gap parameter Δ), the mechanism of Stephen and Bardeen depends on the phase φ of the order parameter since $\mathbf{v}_s(\mathbf{r}) = (\hbar/m)\nabla\varphi$. The two mechanisms therefore appear to be independent. In the local limit the electric field given by (21) has been shown to follow from the microscopic theory.^{16,26} The same electric field also can be derived from the "extra Ginzburg-Landau equation" of Anderson *et al.*²⁷ relating $d\varphi/dt$ to the electrostatic potential. Tinkham, on the other hand, *assumes* a relaxation time $\tau = \hbar/\Delta$, based on a remark by

De Gennes²⁸ that τ should be limited by the uncertainty principle to \hbar/Δ . Anderson²⁹ questions the relevance of this argument and finds $\tau \sim l/v_F (= \tau_{\text{col}})$. In this connection we mention Suhl's recent work¹⁷ which also enables us to estimate the relevant relaxation time. In his treatment of the kinetic energy of a moving fluxoid, the core part involves $[\partial|\psi|/\partial t]^2 = [v_L \partial|\psi|/\partial x]^2$, a process similar to Tinkham's relaxation mechanism. By equating the kinetic energy to $\mu_{\text{core}} v_L^2/2$, he identifies the inertial mass of the vortex core as

$$\mu_{\text{core}} = 3\xi^2 H_c^2 / v_F^2,$$

from which the relaxation time can be derived by the expression

$$\tau = \mu_{\text{core}}/\eta = 3\xi^2 H_c^2 / \eta v_F^2. \quad (24)$$

If we use at low temperatures $H_c^2 = 4\pi N(0)\Delta_{00}$ and η_{emp} given by (15a), then (24) leads to

$$\tau = \left(\frac{3l}{\pi^2 \xi_0} \right) \frac{\hbar}{\Delta_{00}} = \frac{3l}{\pi v_F} \simeq \tau_{\text{col}}. \quad (25)$$

According to this argument the relevant relaxation time is again τ_{col} , which is mean-free-path dependent and for dirty materials is much shorter than that assumed by Tinkham.

Experiments in clean materials may provide a sharper distinction between the two damping mechanisms. Since Tinkham's relaxation time is approximately the time required for an electron to traverse the vortex core, the appropriate τ in the clean limit will be ξ_0/v_F which is still mean-free-path independent.³⁰ On the other hand, the damping mechanism assumed by Stephen and Bardeen arises from the electron collisions in the vortex core, a process that can be significantly modified as l gets larger in comparison with ξ .

IV. HIGH-FIELD SUPERCONDUCTING ALLOYS

The experimental results described in the previous section apply to Nb-Ta and Pb-In alloys for which $\kappa = \lambda/\xi \lesssim 5$ and $H_{c2}(0) \lesssim 10$ kG. In this section we shall be concerned with high-field superconducting alloys such as Nb-Zr, Nb-Ti, and V-Ti, for which κ values range from 10 to over 100.

A. Resistance Minimum

A typical example of flow resistivity measurements on high κ alloys is shown in Fig. 6. One striking feature we note is that in the low-field region the flow resistivity increases as the temperature decreases. In other words, at a given field ρ_f initially decreases as T is increased from zero; combined with the eventual rise in ρ_f at high T this effect produces a minimum in $\rho_f(T)$. For

²⁶ M. J. Stephen and H. Suhl, Phys. Rev. Letters **13**, 797 (1964).

²⁷ P. W. Anderson and A. H. Dayem, Phys. Rev. Letters **13**, 195 (1964); P. W. Anderson, N. R. Werthamer, and J. M. Luttinger, Phys. Rev. **138**, A1157 (1965).

²⁸ P. G. De Gennes, Proceedings of the International School of Physics "Enrico Fermi," Varenna Lectures, 1964 (unpublished).

²⁹ P. W. Anderson (private communication).

³⁰ We owe this remark to P. C. Hohenberg.

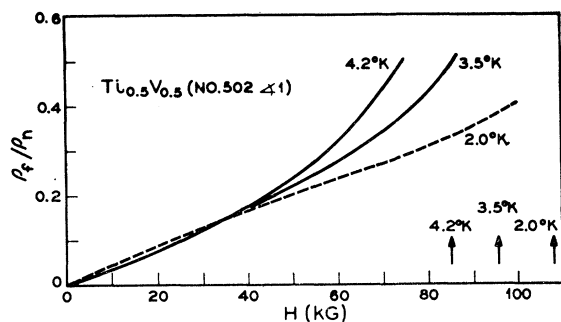


FIG. 6. Flow resistivity of a Ti-V specimen. ρ_f/ρ_n is shown as a function of H at three temperatures. For $H \lesssim 30$ kG, the flow resistivity at 2.0°K shown by the dashed line is larger than that at 4.2°K. The low-field portion of ρ_f/ρ_n for 3.5°K is not shown, but it lies between those for 4.2 and 2.0°K. Vertical arrows indicate the observed upper critical fields.

well-annealed alloys having a small density of defects, this minimum is observable directly in the resistance itself. An example of this phenomenon, which we shall call the "resistance minimum," is illustrated in Figs. 7 and 8. The resistance ratio R/R_n for a well-annealed $\text{Ti}_{0.1}\text{Nb}_{0.9}$ sample is shown as a function of H at two different temperatures. In the low-field region R/R_n is larger at 1.5 than at 4.2°K. R/R_n as a function of T at some fixed H 's is shown in Fig. 8. Note that R decreases as T increases and drops discontinuously as T crosses the λ point of liquid helium. This discontinuity is obviously caused by different cooling conditions below and above T_λ . Because of poorer cooling above T_λ , the specimen temperature rises discontinuously at T_λ . The discontinuous drop in R at T_λ therefore clearly indicates that R is a decreasing function of T in this temperature range.

It should be pointed out that the resistance minimum reported here is a new phenomenon distinctly different from the resistance dips associated with the peak effect. In this sample the peak effect occurs at the transition boundary $H_{c2}(T)$ shown in Fig. 9. If H is increased at a fixed T , then $R(H)$ shows a dip at $H_{c2}(T)$ (e.g., see Fig. 12). If T is increased at a fixed H , then $R(T)$ also

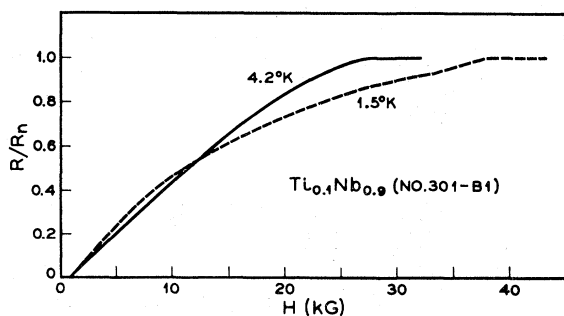


FIG. 7. Resistance versus H for a Ti-Nb specimen. R/R_n as a function of H is shown at two different temperatures. At low fields R is larger at 1.5 than at 4.2°K. This sample is well annealed and contains small amount of defects.

shows a dip at $T_c(H)$.³¹ However, the resistance minima reported here occur in the H - T region far below the transition boundary.

Although the quantitative aspects require further investigations, the occurrence of resistance minima strongly suggests that some sort of spatial nonuniformity is involved in the dissipative mechanism. At $T=0$, the dissipation is probably confined to the vortex-core region, where the conductivity is practically equal to that of the normal state. As T increases, however, the normal-fluid component outside of the core also participates in the dissipation and contributes to the conductivity. Since this additional contribution increases with temperature, it may give rise to an increase in conductance or a decrease in resistance.

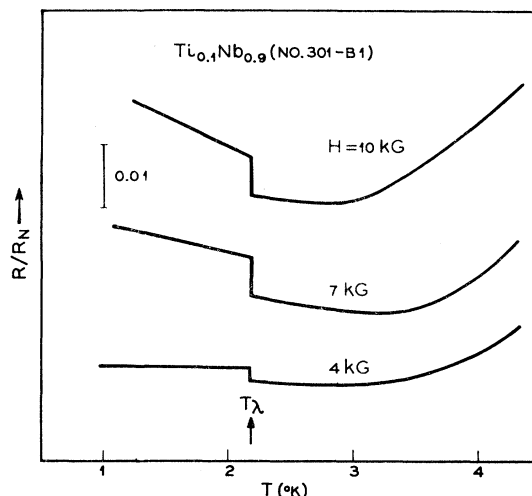


FIG. 8. Resistance minima. R/R_n versus T for the Ti-Nb sample of Fig. 7 is shown at three different fields. R/R_n is relative; the vertical scale shown corresponds to $R/R_n=0.01$. Above T_λ , cooling by the bath liquid helium decreases abruptly and the specimen temperature becomes appreciably higher than the bath. This causes an apparent discontinuity at T_λ when $R(T)$ is plotted as a function of the bath temperature. The residual pinning effect is small for this sample, but is still noticeable particularly in the low-field and low-temperature region.

B. Paramagnetic Effect on H_{c2}

The flow resistivity observed in high- κ alloys does not follow the law of corresponding states unless the observed upper critical fields are corrected for the paramagnetic effect. The pioneering work of Berlincourt and Hake⁴ has convincingly demonstrated that in high- κ alloys the upper critical fields are restricted by the paramagnetic effect predicted by Chandrasekhar³² and by Clogston,³³ rather than by the GLAG mechanism. The flow resistivity, however, reflects primarily

³¹ A dip in $R(T)$ near the peak region was first reported by S. H. Austler, E. S. Rosenblum, and K. H. Goen, Phys. Rev. Letters **9**, 489 (1962).

³² B. S. Chandrasekhar, Appl. Phys. Letters **1**, 7 (1962).

³³ A. M. Clogston, Phys. Rev. Letters **9**, 266 (1962).

Abrikosov's flux structure and in effect can be used as a means of determining $H_{c2}^*(0)$, the GLAG upper critical field that would have been observed in the absence of the paramagnetic effect. The point we would like to make is demonstrated in Fig. 10, where the flow resistivity of a $\text{Ti}_{0.75}\text{V}_{0.25}$ sample is displayed at $t=0.34$ as a function of H . ρ_f/ρ_n increases linearly with H , but only up to $\rho_f/\rho_n \approx 0.3$; then it rises sharply to unity at H_{c2} . If ρ_f/ρ_n of this sample were to behave like that shown in Fig. 4, at $t=0.34$ it would have followed the open line to $H_{c2}^*(t)$. We propose to identify $H_{c2}^*(t)$ as the GLAG upper critical field that would have been observed in the absence of the paramagnetic effect. Thus, we determine $H_{c2}^*(0)$ by extending the straight line portion of $\rho_f/\rho_n(H)$ all the way to $\rho_f/\rho_n=1$. A second-order transition would have occurred at H_{c2}^* as the vortex cores begin to overlap and leave very little superconducting volume. At H_{c2} , however, the vortex cores are still far apart but the superconducting correlation is destroyed by the Pauli spin alignment; the transition therefore may be of first order.

Flow resistivity measurements were carried out systematically in the Ti-V alloy system, for which the most complete data on γ exist³⁴ and $H_{c2}^*(0)$ can be calculated from the GLAG expression (14b). In Fig. 11, $H_{c2}^*(0)$ determined from the flow-resistivity measurements are shown by the open circles; the values of $H_{c2}^*(0)$ calculated from (14b) are shown by the solid line. The good agreement between these two sets of data provides the first "direct" confirmation of the GLAG theory on high- κ alloys. For each alloy com-

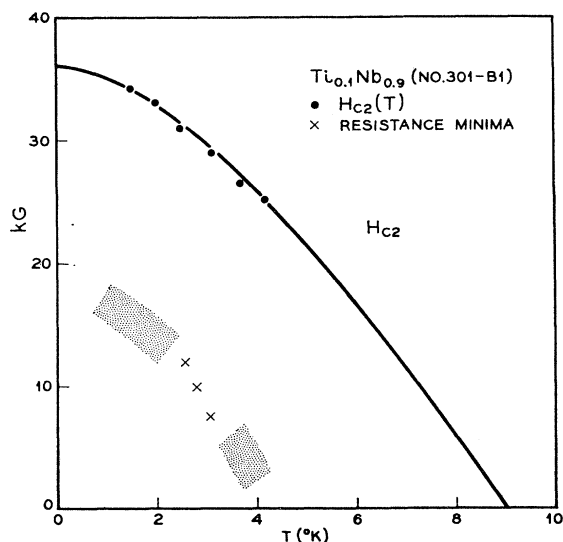


FIG. 9. Locations of the resistance minima in the H_{c2} - T plane. The dots indicate $H_{c2}(T)$ for the Ti-Nb sample of Fig. 7. The observed resistance minima are shown by the crosses; they will probably extend into the shaded region.

³⁴ C. H. Cheng, K. P. Gupta, E. C. van Reuth, and P. A. Beck, Phys. Rev. **126**, 2030 (1962).

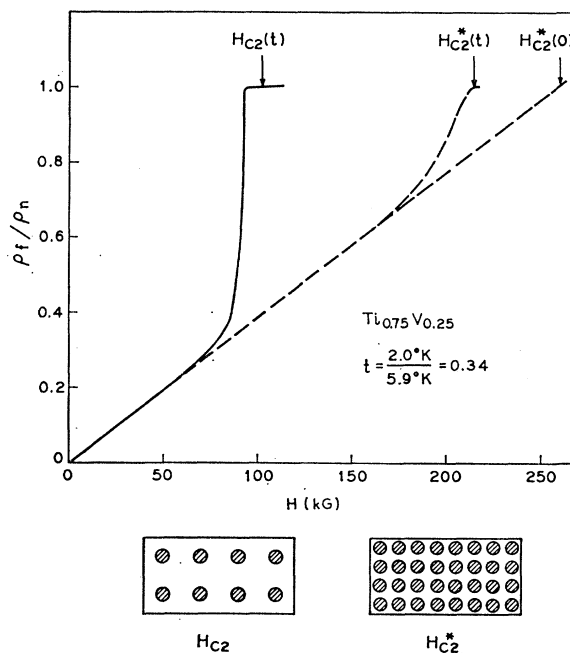


FIG. 10. Paramagnetic effect on the flow resistivity. The measured flow resistivity shown by the solid line increases sharply near $H_{c2}(t)$, the upper critical field restricted by the paramagnetic effect. In the absence of the paramagnetic effect, ρ_f is expected to follow the dashed lines. The inserts show schematically that at H_{c2}^* the cores of flux lines practically overlap, but they are quite far apart at H_{c2} .

position we also obtained $H_{c2}(0)$ by a smooth extrapolation of the measured $H_{c2}(t)$ curves to $t=0$; these are shown by the triangles. The open line shows

$$H_P = \Delta_{00}/\sqrt{2}\mu = 18400T_c, \quad (26)$$

the Clogston field at which the Pauli spin-alignment energy becomes equal to the superconducting gap energy. Finally we show $H_{c2}(0)$ calculated from Maki's expression²⁴

$$H_{c2}(0) = \frac{H_{c2}^*(0)}{(1+\alpha^2)^{1/2}}; \quad \alpha = \frac{\sqrt{2}H_{c2}^*(0)}{H_P}. \quad (27)$$

It is noted that toward the Ti-rich compositions the calculated values of $H_{c2}(0)$ are systematically lower than the observed values. This discrepancy may be due to the spin-orbit interactions, which tends to reduce the paramagnetic effect.³⁵

C. Paramagnetic Effect on the Ratio H_{c3}/H_{c2}

Although this subject is not directly concerned with the flow resistivity, it is included here as it relates to the remarks we made in the preceding paragraph. In the course of measuring the upper critical fields of high-field superconductors, we noted that the ratio

³⁵ K. Maki and T. Tsuneto, Progr. Theoret. Phys. (Kyoto) **31**, 945 (1964).

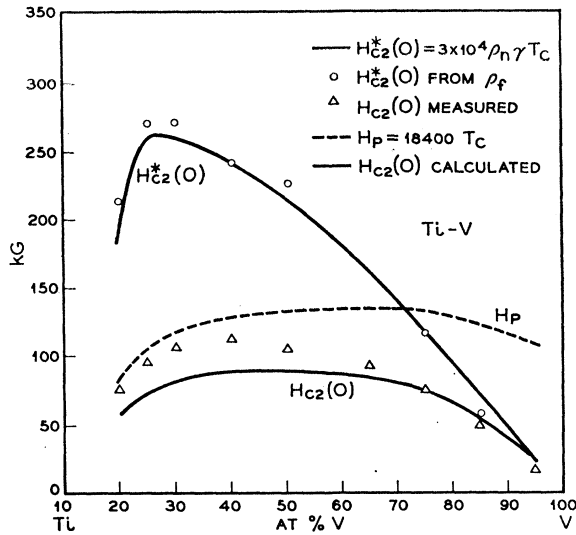


FIG. 11. Upper critical fields of Ti-V system as a function of composition. The open circles indicate $H_{c2}^*(0)$ determined from the flow-resistivity measurements, as in Fig. 10. The solid line is $H_{c2}^*(0)$ calculated from Eq. (14b) of the text. The open line shows H_P calculated from Eq. (26) of the text. The triangles indicate $H_{c2}(0)$ obtained by a smooth extrapolation of the measured $H_{c2}(t)$ to $t=0$. The solid line labeled $H_{c2}(0)$ is calculated from Eq. (27) of the text.

H_{c3}/H_{c2} is typically 1.2 instead of 1.7 that had been theoretically predicted and experimentally observed in low-field type-II superconductors (see Fig. 12). Saint-James and Sarma³⁶ pointed out that this reduction may arise from the paramagnetic effect on H_{c2} and H_{c3} . They simply assumed that the critical-field expression including the paramagnetic effect applies also to H_{c3} . For example, applying (27) to H_{c3} we obtain

$$H_{c3}(0) = \frac{H_{c3}^*(0)}{(1+\alpha^2)^{1/2}}; \quad \alpha' = \frac{\sqrt{2}H_{c3}^*(0)}{H_P} = 1.7\alpha, \quad (28)$$

where H_{c3}^* is the surface critical field in the absence of the paramagnetic effect and hence $H_{c3}^*/H_{c2}^* = 1.7$. From (27) and (28), we obtain

$$\epsilon_m = H_{c3}(0)/H_{c2}(0) = 1.7(1+\alpha^2)^{1/2} \times [1 + (1.7\alpha)^2]^{-1/2}. \quad (29)$$

ϵ_m decreases monotonically with α since the paramagnetic effect always lowers H_{c3} more than H_{c2} . At temperatures close to T_c , Saint-James and Sarma obtained the following expression:

$$\epsilon_s = \frac{H_{c3}(T_c)}{H_{c2}(T_c)} = \frac{\{1 + 2(1.7\alpha)^2\}^{1/2} - 1}{1.7\{(1 + 2\alpha^2)^{1/2} - 1\}}. \quad (30)$$

³⁶ D. Saint-James and G. Sarma, reported at the 1964 Type-II Superconductivity Conference, Cleveland, Ohio (unpublished). Also see C. F. Hempstead, Y. B. Kim, and A. R. Strnad, Bull. Am. Phys. Soc. **10**, 59 (1965).

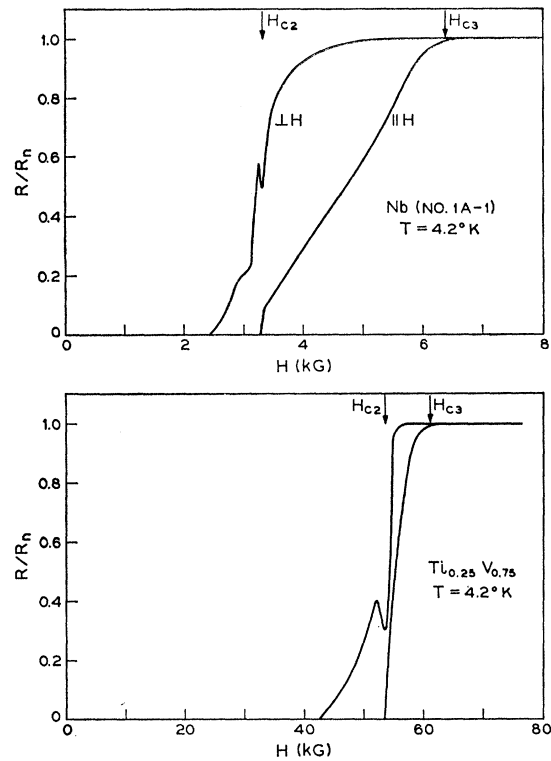


FIG. 12. Determination of upper critical fields by resistive transition. In the parallel orientation, $H \parallel J$ and $H \parallel$ surface, R rises sharply at H_{c2} and approaches to R_n at H_{c3} . When $H \perp J$ and $H \perp$ surface, the specimen shows a dip in R at H_{c2} . Note that H_{c3}/H_{c2} is reduced considerably for the Ti-V sample.

The measured values of H_{c3}/H_{c2} in comparison with these predictions are shown in Fig. 13 for the Ti-V alloy system. For the low values of α the agreement is not too bad, but the disagreement is apparent for large values of α (Ti-rich compositions).

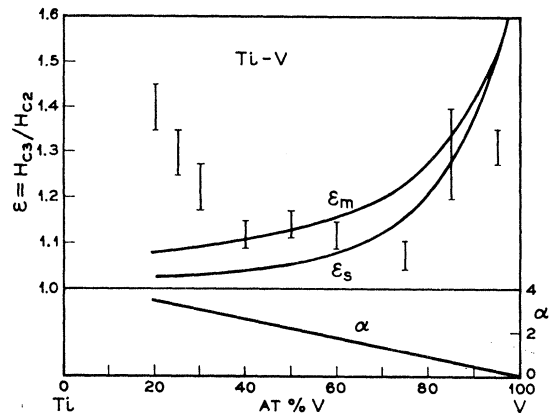


FIG. 13. H_{c3}/H_{c2} of the Ti-V system. The solid lines labeled α , ϵ_m , and ϵ_s are calculated, respectively, from Eqs. (27), (29), and (30) of the text. The measured values are shown by the vertical flags; the errors include the variation among different samples and the variation in temperatures.

V. CONCLUSION

Although the phenomenon involves a nonequilibrium transport process, the electrical resistivity of type-II superconductors has been shown to depend on only a few basic equilibrium quantities. This is in harmony with the original view^{5,11} that the resistive process can be described as a state of "flux flow" in which Abrikosov vortices undergo viscous flow with little distortion in the individual vortex structure. A complete justification of this view must of course await an appropriate time-dependent extension of the GLAG theory.

The following observations indicate that the damping in the medium is closely coupled with the structure of Abrikosov vortices.

(1) The damping effect of the medium is reflected in the flow resistivity, which follows at low temperatures an empirical relation $\rho_f = \rho_n(H/H_{c2})$. Since H/H_{c2} represents the volume fraction of the vortex cores, the empirical result would follow if normal state dissipation takes place only in the vortex-core regions.

(2) This interpretation becomes much more subtle in the case of high-field superconducting alloys. Because of the paramagnetic effect, the upper critical fields H_{c2} observed in these materials are significantly smaller than H_{c2}^* , the upper critical fields predicted from the GLAG mechanism alone. The flow resistivity measured in these materials follows a relation $\rho_f = \rho_n(H/H_{c2}^*)$, indicating that the volume fraction of the vortex cores should be represented more properly by H/H_{c2}^* instead of H/H_{c2} .

(3) The phenomenon of the resistance minimum also reflects the dependence of dissipation on the vortex structure, and is qualitatively accounted for by including the dissipation outside of the vortex core.

As for the dissipative mechanisms that contribute to

the damping, the most obvious one is the induction process. Since the moving magnetic field of a vortex line generates an electric field, dissipative eddy currents are induced in the vortex core. If this process is to account for the observed damping, the magnetic field must be concentrated entirely in the core region. This can be true only near H_{c2} ; at low fields additional damping of much larger magnitude is called for. Stephen and Bardeen¹⁶ argue that the vortex electrons of a moving flux line undergo a cycloidal motion and require an additional electric field. Tinkham,¹⁵ on the other hand, attributes the additional damping to an intrinsic relaxation mechanism associated with a moving flux line. Both models predict a damping close to what observed experimentally.

No evidence is found for the Magnus force on Abrikosov vortices. The effect of damping is already included in the Hall angle expression (7); but the observed effect is several orders of magnitude smaller than predicted by this expression.

In conclusion, the concept of "flux flow" based on the GLAG theory appears to be very effective in accounting for the various aspects of the resistive phenomena of type-II superconductors. It is, however, somewhat disconcerting to realize that so far we have neither a "direct" experimental demonstration that flux lines are moving as envisioned, nor a completely convincing theoretical argument why the flux lines should move as they are described to move.

ACKNOWLEDGMENTS

We are indebted to R. Epworth and J. Hasiak for technical assistance. We have benefited greatly from our discussions with P. W. Anderson, P. C. Hohenberg, M. J. Stephen, and N. R. Werthamer.